J Radioanal Nucl Chem (2017) 311:1917–1921
DOI 10.1007/s10967-017-5170-9

Radiation damage induced in Zircaloy-4 by 2.6 MeV proton irradiation

M. Izerroukenn[1] · O. Menchi[1] · A. Sari[2] · W. Djerourou[3] · H. Medjkoun[1]

Received: 17 October 2016 / Published online: 6 January 2017

Abstract Radiation damage induced in Zircaloy-4 by 2.6 MeV proton irradiation at low doses was studied. Our aim is to emulate the effect of neutron irradiation during early stages of irradiation. X-ray diffraction analysis reveals that the domain size remains constant, while the microstrain increases after irradiation to a dose of 0.017 dpa. The micro-hardness, nano-hardness and Young's modulus are found to decrease after irradiation to a dose of 0.017 dpa. These indicate, respectively, the formation of a high concentration of point defects, probably vacancy type, and a decrease in the second phase precipitates size.

Keywords Zircaloy cladding material · Dislocation loops · Vacancy type defects · Micro-indentation method

Introduction

Zirconium alloys are widely used in nuclear technology as fuel cladding, structural materials and pressurize pipe due to their interesting properties. It exhibits a good resistance to radiation damage, good corrosion resistance and very low thermal neutron absorption cross section. Proton-induced damage in structural materials has been extensively investigated in the past decade in order to emulate the neutron irradiation effects [1–9]. It was found that proton and neutron irradiation produce comparable mechanical and structural properties behavior [10–12]. However, most of these investigations were conducted at high temperature (300–350 °C) and high dose. For author's knowledge, there has been very little research reported on Zircaloy-4 behavior under low irradiation doses. Although, such data are needed to understand the defect formation during the early stage of irradiation. The purpose of the present study is therefore to ascertain the defects structure induced in Zircaloy-4 at low irradiation dose. The main goal of the present work has been to emulate the neutron effects during early stage of irradiation. However, we are also interested to estimate the contribution of protons injected in cladding by fast neutron elastic collision with hydrogen atom of the reactor coolant water to the total aging associated with degradation. The latter process is not dominant, but significant. Nauchi and Kameyama [13] have estimated for the first time the number of protons injected into LWR fuel cladding materials using MCNP and SRIM codes. They have found that the increment of hydrogen content in claddings by such process is estimated to 5 ~ 12 wt-ppm at 40 MWd/kgHM burn-up for boiling water reactor operating conditions.

Note that the hydrogen uptake by Zircaloy due to the corrosion under research reactor operating conditions (~ 60 °C) is insignificant. Therefore, the present study includes proton-induced damage in pre-hydrided Zircaloy with hydrogen content lower than 70 ppm as can be found in cladding of nuclear research reactor. Furthermore, due to the high scattering cross section recoil proton with energy of 2 MeV may induce high displacement defects along their path which affect the mechanical and structural

✉ M. Izerroukenn
izerrouken@yahoo.com

[1] Nuclear Research Center of Draria, BP 43 Sebbala, Draria, Algiers, Algeria

[2] Nuclear Research Center of Birine, BP 108, Ain-Oussera, Djelfa, Algeria

[3] Faculty of Physics, University of Science and Technology Houari Boumediene, BP 32, Al-Alia, Bab-ezouar, Algiers, Algeria

properties of the core structural components. In the present study X-ray diffraction (XRD) has been used to study the structural and microstructural properties evolution. Mechanical tests were also conducted to evaluate the hardness and Young's modulus.

Experimental

The sample investigated in this study is a recrystallized Zircaloy-4 sheet with a thickness of about 2 mm. The chemical composition of the main elements is 1.6 wt% Sn, 0.21 wt% Fe, 0.08 wt% Cr, 0.1 wt% O, 0.29 wt% (Fe+Cr) and 97.7 wt% Zr. Small pieces with size of about 5 mm × 5 mm, were cut from the same zirconium plate by a diamond saw. The sample is noted Zy-4. Sample hydriding was carried out using hydride equipment at 400 °C. Because the study is devoted to structural material used in the research reactor, the hydrogen content introduced is lower than 70 ppm. The sample is noted (H-Zy).

2.6 MeV proton beam irradiation was performed at iThemba LABS, South Africa using Van de Graaff accelerator. The irradiations were carried out at room temperature in a vacuum chamber at 5×10^{-6} mbar with proton flux of 10^{13} p/cm^2 s. The ion beam was focused to a diameter of 6 mm. The displacement damage calculated using SRIM 2003 code with displacement energy of 40 eV and using the "Quick" Kinchin and Pease damage calculation is shown in Fig. 1 [14]. The maximum damage (peak damage) is induced at depth of about 43 μm corresponding to the projected range of 2.6 MeV protons in zirconium. The number of displacement per atom (n_{dpa}) was calculated using Eq. (1) [15].

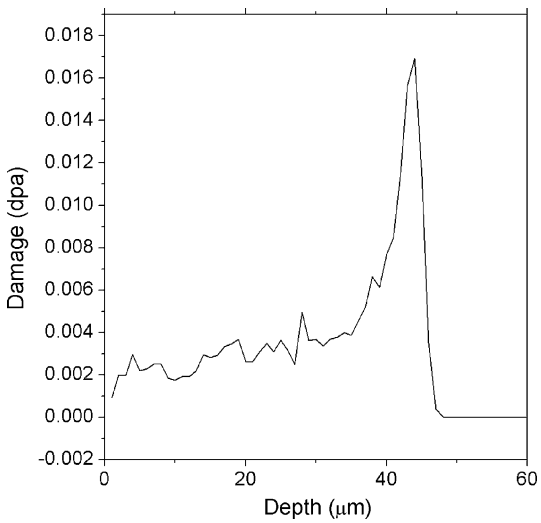

Fig. 1 SRIM calculations of n_{dpa} for 2.6 MeV protons at fluence of 10^{17} p/cm^2

$$n_{dpa} = \frac{\phi \cdot N_d \cdot A}{\rho \cdot d \cdot N_A} \quad (1)$$

where ϕ is the proton fluence, N_d is the number of displacements per ion, A is the molecular mass of the target material, ρ is the density, d is the penetration depth, N_A is Avogadro's number. The n_{dpa} at peak damage corresponding to proton fluences of 10^{16} and 10^{17} p/cm^2 are, 0.0017 and 0.017 dpa, respectively.

Characterization methods

After irradiation the structure modifications are observed using XRD, X' PERT PRO MPD in the Bragg–Brentano geometry: the X-ray source was a copper tube ($CuK_\alpha = 1.540{,}598$ Å) and a PIXcel 1D detector was used for X-ray detection. The 2θ scan range was 20°–80° with a step size of 0.026°. The mechanical tests were performed using micro-durometer MHT 10, Zeiss and nano-indenter CSM instruments at room temperature. Micro-hardness measurements were performed using Vickers indenter with loads of 1 N (100 g) and load time of 5 s. Nano-indentation measurements (nano-hardness and Young's modulus) were made using Berkovich indenter with load of 0.3 N (30 g) and load time of 10 s. The micro-hardness, nano-hardness and Young's modulus values were measured using similar method adopted by Yan et al. [9], where seven indentations were tested for each experiment parameter. The maximum and minimum values were removed, and the average of residual five indentations was taken for each experiment parameter. Before analyses, the samples were submitted to fine polishing and then chemically etched in 10% HF + 45% HNO_3 + 45% distilled water.

Results and discussion

Structural analysis

Figure 2 shows the XRD patterns of Zy-4 and H-Zy samples before irradiation. The main observed diffraction peaks at $(0002), (00\bar{1}1), (10\bar{1}2), (10\bar{1}3), (0004)$ correspond to the α-Zr hcp phase. As can be seen, from the XRD pattern, all diffraction peaks are little bit shifted towards lower diffraction angle in the case of the H-Zy sample compared to the Zy-4. An example of the (0002) peak shift is shown in the inset. This indicates the expansion of the hexagonal lattices due to the hydrogen interstitial atoms [16]. According to Williamson-Hall (W-H) technique, the line broadening is due to the contribution of small particle size and microstrain [17]. Using this approach, the integral

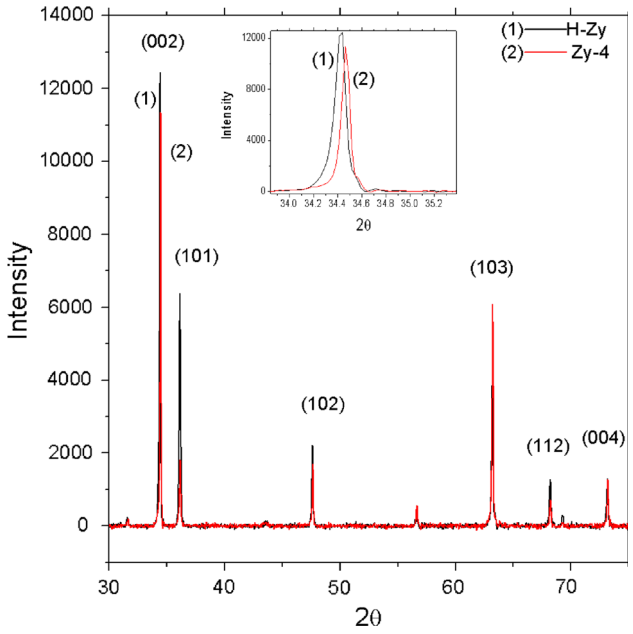

Fig. 2 XRD patters of Zy-4 and H-Zy samples before irradiation. The *inset curve* show the shift of (002) peak position of H-Zy sample compared to the Zy-4 one

breath β is related to the domain size D_v and microstrain ε by:

$$\frac{\beta\cos(\theta)}{\lambda} = \frac{1}{D_v} + 4\varepsilon\left(\frac{\sin(\theta)}{\lambda}\right) \quad (2)$$

where θ is the Bragg angle. A plot of $(\beta\cos(\theta)/\lambda)$ as a function $4(\sin(\theta)/\lambda)$ (Fig. 3) gives the domain size and microstrain. The obtained results are reported in Table 1. From the Table 1, one can see that the domain size is

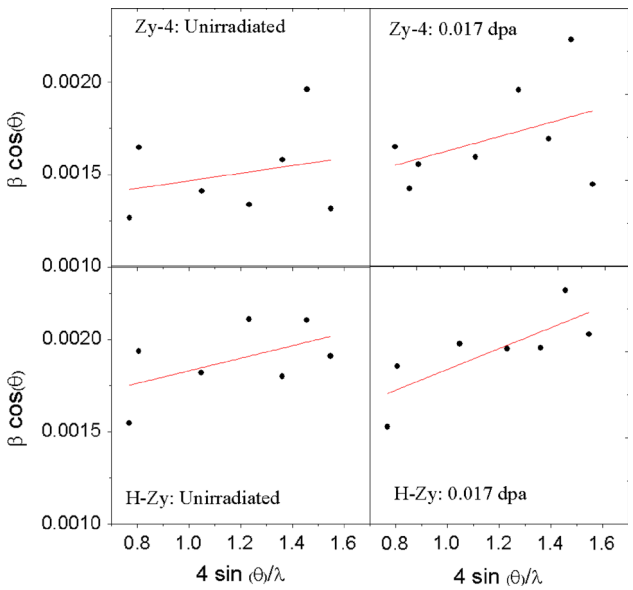

Fig. 3 W–H plot for virgin and irradiated Zy-4 and H-Zy samples

Table 1 Microstress and domain size values determined from W–H plots

Dose (dpa)	D_v (Å)		ε (%)	
	Zy-4	H-Zy	Zy-4	H-Zy
Unirradiated	794	671	2.1×10^{-4}	3.4×10^{-4}
0.0017	694	–	3.1×10^{-4}	–
0.017	758	775	3.8×10^{-4}	6.0×10^{-4}

almost constant after 2.6 MeV proton irradiation. While the microstrain increases for both Zy-4 and H-Zy samples due to the point defects formation, probably vacancy types. Indeed, the strain fields induced around the vacancy due to the atomic bond compression may explain the microstrain increase. However according to Kai et al. [2] data, the second phase particles size (SPP's) decreases when Zircaloy-4 is irradiated by 1 MeV proton to low dose (0.01 dpa). It is worthwhile to notice that the microstrain corresponding to H-Zy sample is higher than that of Zy-4. This means that the presence of Hydrogen atom in interstitial position induces additional stress.

Mechanical properties

Micro-hardness of Zy-4 and H-Zy samples before and after irradiation is depicted in Fig. 4. From this figure one can see that the micro-hardness values of both Zy-4 and H-Zy decreased a little bit after irradiation to a dose of 0.017 dpa. It is reduced with about 6% for Zy-4 and 4% for

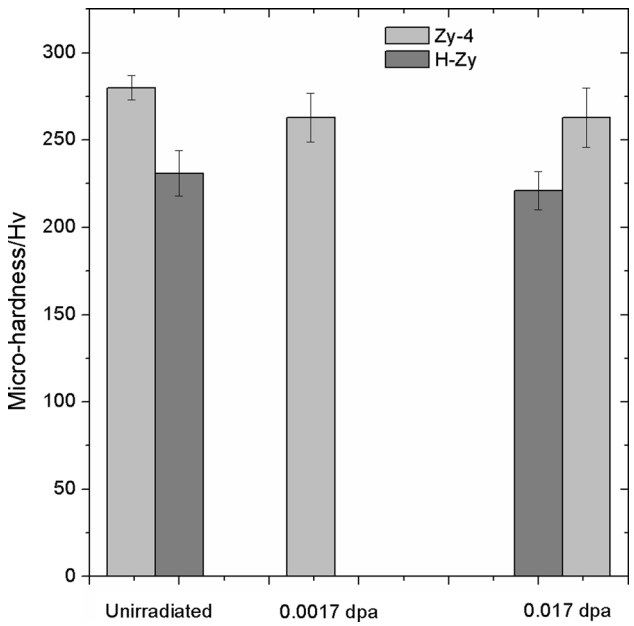

Fig. 4 Micro-hardness of Zy-4 and H-Zy before and after 2.6 MeV proton irradiation

H-Zy compared to the initial value of 280 and 230 Hv respectively. It is found from earlier findings that micro-hardness increases when Zircaloy-4 is irradiated by 2 MeV proton at high doses (>1 dpa) [7].

Nano-indentation measurements given nano-hardness and Young's modulus as a function of dose are presented in Fig. 5. As can be seen, nano-hardness and Young's modulus decreased after irradiation for both Zy-4 and H-Zy samples in accordance with the micro-hardness results. The average nano-hardness is reduced from 2.57 to 2.37 GPa for Zy-4 sample (a decrease of 8%), and from 2.39 to 2.35 GPa for H-Zy sample (a decrease of 2%). The Young's modulus of Zy-4 and H-Zy samples before irradiation are respectively, 97 and 91 GPa. These values reduced to 72 GPa for Zy-4 sample (a decrease of 26%) and to 79 GPa for H-Zy sample (a decrease of 12%) after irradiation to a dose of 0.017 dpa. As can be seen the variation of Young's modulus is more important compared to the nano-hardness indicating that damage structure generated by 2.6 MeV proton irradiation is dominated by point defects in accordance with XRD results. Indeed it is known that Young's modulus is closely related with the atomic bonding and crystal structure [18]. It is worthy to note that the relative reduction in the micro-hardness, nano-hardness and Young's modulus compared to the unirradiated sample is lower for H-Zy sample than that of Zy-4. This indicates that the rate of reduction of hardness upon irradiation is lower in the case of pre-hydrided zircaloy due to the presence of hydrogen interstitial defects.

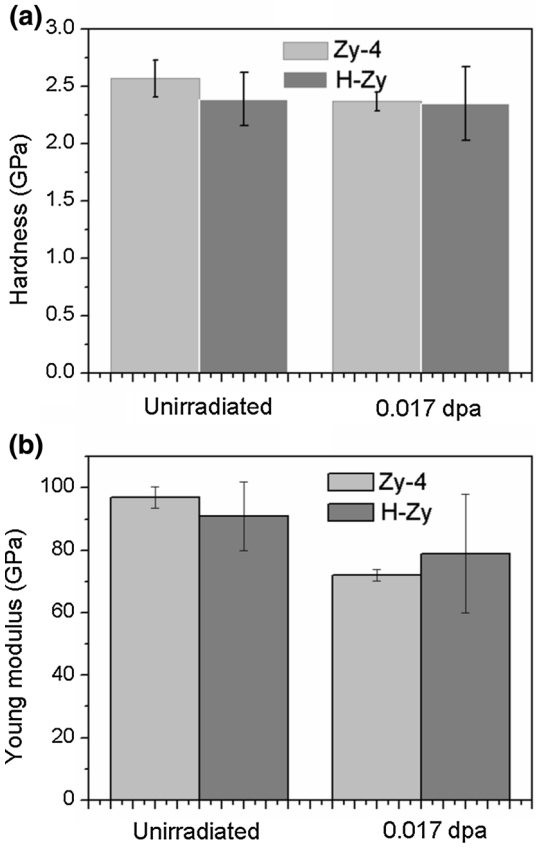

Fig. 5 Nano-hardness (**a**) and Young's modulus (**b**) of Zy-4 and H-Zy samples before and after 2.6 MeV proton irradiation

Discussion

Energetic incident particle induces high point defects (vacancies and interstitials) concentration along their path in structural materials. At high irradiation doses, when, the point defects become supersaturated, vacancy and interstitial clustering occur and collapse into voids and dislocation loops. These lead to the microstructure and mechanical properties changes. The microstructure modifications induced by ion irradiation in structural materials have been investigated in numerous papers. Most of the authors agreed that the microstructure modification such as domain size is due to the dislocation loops formation [19–21]. In contrast, the irradiation induced hardening mechanism in structural material is not well understood. In ceramic materials the irradiation hardening is caused by the point defects and small defect clusters see Ref. [22] and reference therein. Jagielski et al. [23] attributed the hardness changes in 320 keV Kr-irradiated sapphire to the total amount of accumulated damage, whereas, the Young's modulus to the amorphization of the crystalline structure. Recently, Yan et al. [21] suggested that the hardness changes observed in 6.37 MeV Xe^{26+} ions irradiated Zr-1Nb is due to the contribution of microstructure of dislocation loops, vacancy-type defects and SPP's. Moreover, Kai et al. [2] found that the $Zr(Fe, Cr)_2$, (hcp) phase was gradually dissolved after irradiation to a dose of 0.01 dpa in 1 MeV proton irradiated Zircaloy-4. Above the latter dose a new $Zr(Fe, Cr)_2$, (fcc) phase was formed and grown to a larger size. This behavior is consistent with the hardness evolution observed in the present study at low dose (0.017 dpa) and Zu et al. [7] results at high dose (>1 dpa). Therefore, it can be suggested that the SPP's size contribute significantly to the Zircaloy-4 hardening.

Conclusions

Zircaloy-4 fuel cladding materials as well as pre-hydrided Zircaloy-4 at about 70 ppm were bombarded with 2.6 MeV protons at low dose (0.017 dpa). The resulted radiation damage was characterized using XRD techniques. Radiation hardening was also investigated using micro-indentation and nano-indentation tests. The irradiations induce microstrain increase without change in the domain size.

This explains that the irradiated microstructure at low dose is dominated by the point defects, probably vacancy-type. It is found from mechanical tests that the micro-hardness, nano-hardness and Young's modulus is reduced after irradiation at low doses.

Taking into account Kai et al. [2] results, the hardness decrease is attributed to the decrease of the SPP's size. Thus, we suggest that the SPP's size contribute significantly to the Zircaloy-4 hardening change. According to this experimental data, three main conclusions may be addressed: (i) during the early stage of irradiation, the second phase precipitates size decreases. Further study using transmission electronic microscopy (TEM) is needed to confirm the result. (ii) The hydrogen uptake by Zircaloy-4 even in a small quantity influences the crystalline structure and defects microstructure. (iii) Taking into account Nauchi and Kameyama results, where the recoil process is a part of hydrogen absorption mechanism of light-water reactor (LWR) fuel cladding, it is necessary to consider the defect generated by recoil protons in the aging management of core structural material.

Acknowledgements This work is performed in frame of the CRP project: Establishment of Material Properties Database for Irradiated Core Structural Components for Continued Safe Operation and Lifetime Extension of Ageing Research Reactors. IAEA Research contract N° 17881. The authors are indebted to Prof. M. Maaza for Protons irradiation.

References

1. Lucas GE, Surprenant M, Dimarzo J, Brown GJ (1981) Proton irradiation creep of Zircaloy-2. J Nucl Mater 101:78–91
2. Kai JJ, Huang WI, Chou HY (1990) The microstructural evolution of Zircaloy-4 subjected to proton irradiation. J Nucl Mater 170:193–209
3. Cann CD, So CB, Styles RC, Coleman CE (1993) Precipitation in Zr-2.5 Nb enhanced by proton irradiation. J Nucl Mater 205:267–272
4. Was GS, Allen TR, Busby JT, Gan J, Damcott D, Carter D, Atzmon M, Kenik EA (1999) Microchemistry and microstructure of proton-irradiated austenitic alloys: toward an understanding of irradiation effects in LWR core components. J Nucl Mater 270:96–114
5. Was GS, Busby JT, Allen T, Kenik EA, Jensson A, Bruemmer SM, Gan J, Edwards AD, Scott PM, Anderson PL (2002) Emulation of neutron irradiation effects with protons: validation of principle. J Nucl Mater 300:198–216
6. Chow CK, Holt RA, Woo CH, So CB (2004) Deformation of zirconium irradiated by 4.4 MeV protons at 347 K. J Nucl Mater 328:1–10
7. Zu XT, Sun K, Atzamon M, Wang LM, You LP, Want FR, Busby JT, Was GS, Adamson RB (2005) Effect of proton and Ne irradiation on the microstructure of Zircaloy 4. Philos Mag 85:649–659
8. Shen HH, Peng SM, Xiang X, Naab FN, Sun K, Zu XT (2014) Proton irradiation effects on the precipitate in a ZR-1.6n-0.6Nb-0.2Fe-0.1Cr alloy. J Nucl Mater 452:335–342
9. Yan C, Wang R, Wang Y, Wang X, Bai G (2015) Effects of ion irradiation on microstructure and properties of zirconium alloysd a review. Nucl Eng Technol 47:323–331
10. Francis EM, Harte A, Frankel P, Haigh SJ, Jädernäs D, Romero J, Hallstadius L, Preuss M (2014) Iron redistribution in a zirconium alloy after neutron and proton irradiation studied by energy-dispersive X-ray spectroscopy (EDX) using an aberration-corrected (scanning) transmission electron microscope. J Nucl Mater 454:387–397
11. Tournadre L, Onimus F, Béchade JL, Gilbon D, Cloué JM, Mardon JP, Feaugas X, Toader O, Bachelet C (2012) Experimental study of the nucleation and growth of c-component bloops under charged particle irradiations of recrystallized Zircaloy-4. J Nucl Mater 425:76–82
12. Tournadre L, Onimus F, Béchade JL, Gilbon D, Cloué JM, Mardon JP, Feaugas X (2013) Towards a better understanding of the hydrogen impact on the radiation induced growth of zirconium alloys. J Nucl Mater 441:222–231
13. Nauchi Y, Kameyama T (2011) Modeling of H (n, n) recoil proton injection into LWR fuel cladding with sequential use of MCNP and SRIM codes. Prog Nucl Sci Technol 2:101–106
14. Ziegler F, Biersack JP, Littmarck U (1985) The stopping and range of ions in solids, Pergamon, New York. http://www.srim.org/
15. Hengstler-Eger RM, Baldo P, Beck L, Dorner J, Ertl K, Hoffmann PB, Hugenschmidt C, Kirk MA, Petry W, Pikart P, Rempel A (2012) Heavy ion irradiation induced dislocation loops in AREVA's M5® alloy. J Nucl Mater 423:170–182
16. Vizcaino P, Santisteban JR, Vicente Alvarez MA, Banchik AD, Almer J (2014) Effect of crystallite orientation and external stress on hydride precipitation and dissolution in Zr2.5%Nb. J Nucl Mater 447:82–93
17. Williamson GK, Hall WH (1953) X-ray line broadening from filed aluminium and wolfram. Acta Metall 1:22–31
18. Egeland GW, Valdez JA, Maloy SA, McClellan KJ, Sickafus KE, Bond GM (2013) Heavy-ion irradiation defect accumulation in ZrN characterized by TEM, GIXRD, nanoindentation, and helium desorption. J Nucl Mater 435:77–87
19. Neogy S, Mukherjee P, Srivastava AP, Singh MN, Gayathri N, Sinha AK, Srivastava D, Dey GK (2015) Proton irradiation of Zr-1 wt% Nb cladding material: a depth-wise assessment of inhomogeneous microstructural damage using X-ray diffraction line profile analyses. J Alloy Compd 640:175–182
20. Sarkar A, Mukherjee P, Barat P (2008) Effect of heavy ion irradiation on microstructure of zirconium alloys characterized by X-ray differaction. J Nucl Mater 372:285–292
21. Yan C, Wang R, Wang Y, Wang X, Bai G, Zhang Y, Lu E, Wang B (2015) Effet of Xe^{26+} ion irradiation on the microstructural evolution and mechanical properties of Zr-1 Nb at room and High temperature. J Nucl Mater 461:78–84
22. Yang Y, Dickerson CA, Allen TR (2009) Radiation stability of ZrN under 2.6 MeV proton irradiation. J Nucl Mater 392:200–205
23. Jagielski J, Thomé L, Nowicki L, Turos A, Gentils A, Garrido F, Piatkowska A, Aubert P (2005) Ion irradiation of ceramic oxides: disorder production and mechanical properties. Nucl Instrum Methods B 240:111–116